Al-Khwarizmi Engineering Journal, Vol. 19, No. 4, December, (2023)
P. P. 78- 89

Al-Khwarizmi Engineering Journal

PDF Comparison based on Various FSO Channel Models under Different Atmospheric Turbulence

Mahdi A. Atiyah* Lwaa Faisal Abdulameer**
Gaurav Narkhedel***

*,***Department of Information and Communication/Al-khwarizmi College of Engineering/ University of Baghdad/ Iraq*
**** School of Electronic and Communication Engineering/ Dr Vishwanath Karad MIT World Peace University/ India*
Corresponding Author*Email: mahdi.abd2103m@kecbu.uobaghdad.edu.iq
** Email: lwaa@kecbu.uobaghdad.edu.iq
***Email: ggnarkhede9@gmail.com

(Received 9 April 2022; accepted 28 September 2023)
https://doi.org/10.22153/kej.2023.09.004

Abstract

Recently, wireless communication environments with high speeds and low complexity have become increasingly essential. Free-space optics (FSO) has emerged as a promising solution for providing direct connections between devices in such high-spectrum wireless setups. However, FSO communications are susceptible to weather-induced signal fluctuations, leading to fading and signal weakness at the receiver. To mitigate the effects of these challenges, several mathematical models have been proposed to describe the transition from weak to strong atmospheric turbulence, including Rayleigh, lognormal, Málaga, Nakagami-m, K-distribution, Weibull, Negative-Exponential, Inverse-Gaussian, G-G, and Fisher-Snedecor F distributions. This paper extensively studies and analyses different probability density functions (PDFs) that govern the FSO channel, considering various channel models. This paper aims to comprehensively understand how FSO channels can be effectively modeled using different PDFs. Accurate modeling is crucial for designing FSO systems that can operate optimally under potential environmental conditions. Selecting the appropriate PDF model plays a crucial role in determining the FSO channel's performance during system design. With a multitude of PDF models available, this study aims to identify the most effective PDF model to be employed in FSO channel modeling.

Keywords: *Atmospheric Turbulence (AT), Fisher-Sedecor F, FSO, Gamma-Gamma(G-G) lognormal(LN), PDF.*

1. Introduction

High bandwidth, speed, low power usage, and virtual reality are some of the increasing connectivity requirements that 5G should have to address [1]. FSO is a promising candidate to meet the requirements of high capacity and sufficient speed in 5G and beyond. However, line-of-sight (LOS) is essential in implementing the FSO link. Therefore, planes and trees are considered obstacles and limitations. In addition, atmospheric turbulence (AT) (fog and rain) mainly affects the quality of FSO [2]. Since Device-to-Device (D2D) enables direct connections without requiring a foundational management network. (D2D) is a leading candidate to meet the requirements of the fifth generation [3]. In addition to improving system security, FSO's use of an unlicensed optical frequency allows for its operation. FSO is a form of airborne broadband communication that involves the transmission of coherent visible or infrared light. [4]

High-spectrum efficiency in wireless optical communication was improved by employing the (MIMO) technique. [5,6]. Accuracy and simplicity of complexity are essential in achieving beneficial results in knowing the effects of the channel on the FSO binding[7].

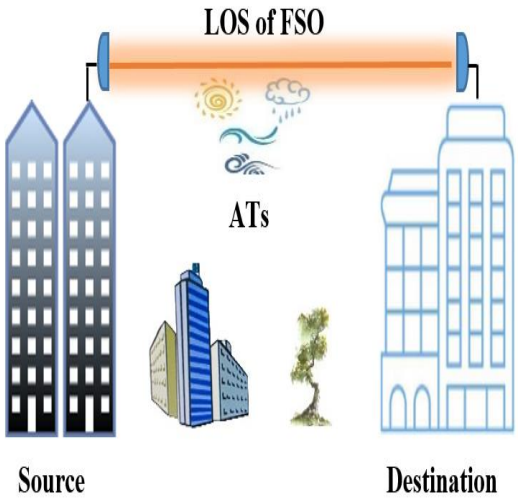

Fig. 1. Environmental of FSO with ATs.

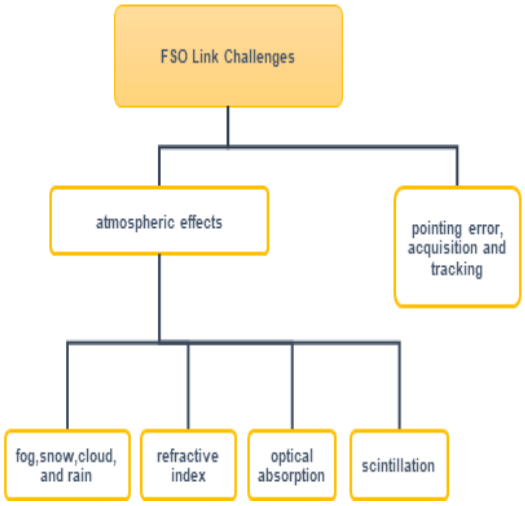

Fig. 2. Challenges Encountered in FSO System.

Atmospheric effects and PE represent the biggest challenge to the quality of communication. Scintillation occurs due to air turbulence, a well-known issue connected to the channel's weather. Moreover, the efficacy of the link is greatly affected by spatial jitter, which occurs due to occasional misalignments between the transmitter and the receiver. The term for this is PE [8]. A PDF distribution is also impacted by the aperture averaging effect, which tends to lessen the harmful impacts of scintillation and turbulence [9].

2. Related Work

For FSO-based data transmission between two devices, LOS is required. The optical signal is significantly affected by attenuation caused by weather conditions, and its effect increases with the distance between the two devices [10]. It is a fundamental challenge with significant implications for the design of FSO links [11]. To reduce the bit error rate (BER) of the FSO link in opposite ATs. In a FOS link, electric fields in the atmosphere affect signal transmission. [12].

Scintillation caused by intensity and phase changes in the channel is the main source of noise in an FSO communication system. The PDF of the received irradiance of the optical field satisfies design parameters like detector threshold level, probability of detection, mean fade time, number of fades, and SNR [13]. The main factor in determining AT strength is the air's refractive index structure parameter (C_n^2) [14]. See Figure 2.

The turbulence is differentiated into three cases: weak ($C_n^2 = 10^{-17}m^{-2/3}$), moderate ($C_n^2 = 10^{-14}m^{-2/3}$), and strong ($C_n^2 = 10^{-13}m^{-2/3}$). The combination of the transmitted light signal and the atmospheric channel impulse response is the signal that is taken by the receiver. The consequences of channel distortion are examined using the impulse response. [13]

Many basic models are proposed in the channel characterization of FSO communication by analyzing system parameters and inferring what is observed in the PDF value.

The Rayleigh distribution was used to model the FSO communication channel, which was analyzed and verified experimentally using PDF for weak AT [15]. The fading associated with the weak atmospheric turbulence regime is typically modeled using the log-normal distribution [16].

In [17], the atmospheric environment and PE are essential factors in FSO connection quality limitations. G-G is used to investigate FSO channel parameters with pointing errors. A G-G distribution has been used to characterize FSO connectivity among ATs to evaluate system performance for moderate turbulence [18]. The efficiency of an FSO channel was compared (in 2019) using the G-G and negative exponential (NE) models[19].

The authors of [20] have recently proposed a new Fisher- Snedecor (F model) turbulence distribution model to characterize AT over FSO interconnections. Also, in [7], an F model is proposed in the characterization of channel perturbation in FSO communication.

Compared to the LN and G-G models, the proposed F turbulence distribution model in [2]

better matches experimental data for all turbulence conditions. Furthermore, the F turbulence distribution is mathematically more straightforward than other distributions, such as the G-G, LN, and M distribution, because the PDF of the F distribution contains fundamental elementary functions analyzing FSO communication systems. F model can analyze the FSO system under various disturbance conditions.

The Málaga (M) distribution is more general in describing various perturbation states of the channel when steering errors are considered a robust statistical model in the expression. In contrast, distribution models such as the natural logarithm, G-G, and k distribution describe weak, medium, and strong perturbations. In [21], closed expressions are provided for the rate code error and potential outage. The M distribution is used in [22] to simulate the FSO channel. The surface radiation fluctuation of infinite optical signals is described by a statistical model that has gained prominence recently. M distribution is a thorough model considering all AT, from weak to strong disturbances. Although the M distribution can model weak-to-strong AT fluctuations, it is less capable of arithmetic tracking, as it is more complex than the G-G model. [23]

In [24], Weibull distribution was used to evaluate the performance of FSO under water and proved that it has a high ability to correspond with the experimental results of the simulation. In [25], the F distribution was used to analyze a combined millimetre wave (mm-wave) and FSO system with appropriate channel parameters. Although the F model is the most suitable and traceable due to its computational availability for modeling the FSO communication channel compared to the G-G model. It was considered the simplest mathematically in terms of complexity. [2] However, the G-G model is the most convenient and widely used because it works in all types of ATs. The F model was applied on a double-hop FSO channel with the G-G model, and the simulation obtained almost identical results for both models. [26]

The PDF tails mostly determine the precision of signal recognition and fading probability [15]. The received irradiance PDF is nonstationary and is highly dependent on atmospheric turbulence factors. Nonetheless, an exact PDF of the received irradiance is required to construct a robust and dependable FSO communication system. In the next section, the channel analysis of the proposed selects the best suitable model under different conditions depending on the simulation results.

3. System and Channel Model

Any modeled channel is based on atmospheric turbulence. In FSO communication, the channel is considered an atmosphere. By changing important factors like beam divergence, modulation techniques, MIMO techniques, future ultimately, etc., constructing a more effective FSO system can help to increase bit rate, transmission distance, and gain[16].

3.1 Rayleigh Distribution

The Rayleigh (R) distribution was used to analyze the channel gain in FSO communication by extracting the PDF value. It was observed that the scintillation index is 1. The density function of the R-distribution is more concentrated at low values. [13]. The PDF of the R distribution is given as:

$$P(I_o)_{Rd} = \frac{1}{\sigma_R^2}\exp\left(\frac{-I_o}{2\sigma_R}\right), I_o > 0 \quad \ldots(1)$$

Where σ_R^2 is the Rytov variance.

3.2 Lognormal and Gamma-Gamma Distributions

The feeble regime of AT is described using an LN distribution model. However, the G-G distribution model is also presented to characterize the turbulent channel, as it has been demonstrated to provide high accuracy under moderate-to-strong conditions. [27]. The LN model is the most popular AT model because of its comparatively straightforward shape [9].

Scintillation is the temporal and spatial fluctuation of light intensity induced by turbulent atmospheric conditions. When normalized, the scintillation index is defined as the variance of the light wave intensity [14]. According to [27], the half peak of the light intensity (I_o) is an identically distributed Gaussian random variable with a mean zero and a variance σ_o^2. By PDF of an LN distribution can be expressed as:

$$P(I_o)_{LN} = \frac{1}{I_o\sqrt{2\pi\sigma_o^2}}\, e^{\left(-\frac{(\ln I_o + \frac{\sigma_o^2}{2})^2}{2\sigma_o^2}\right)} \quad \ldots(2)$$

Where σ_o^2 (Rytov variance) can be calculated as: [14]

$$\sigma_o^2 = 1.23 C_n^2 K^{\frac{7}{6}} d^{\frac{11}{6}} \quad \ldots(3)$$

Where $k = {}^{2n}/_{\lambda}$ is a wave number, λ is the wavelength of the transmitter, and d is the link distance [28]**.** Under signal transmission in moderately strong conditions, the PDF of the G-G model can be expressed as: [27]

$$P(I_o)_{GG} = \frac{2(\alpha_o\beta_o)^{\frac{\alpha_o+\beta_o}{2}}}{\Gamma(\alpha_o)\Gamma(\beta_o)}.$$

$$I_o^{\frac{\alpha_o+\beta_o}{2}-1} B_{\alpha_o-\beta_o}(2(\alpha_o\beta_o I_o)^{0.5}) \quad \ldots(4)$$

Where $\Gamma(.)$ Gamma function, $B_i(.)$ is a Bessel function of the second kind, and in the *i*-th order, α_o and β_o are the effective turbulence at small and large scales **as:** [14]

$$A_o = \left[\exp\left(\frac{0.49\,\sigma_o^2}{(1+1.11\sigma_o^{\frac{12}{5}})^{7/6}}\right) - 1\right]^{-1} \quad \ldots(5)$$

$$\beta_o = \left[\exp\left(\frac{0.5\,\sigma_o^2}{(1+0.69\sigma_o^{\frac{12}{5}})^{5/6}}\right) - 1\right]^{-1} \quad \ldots(6)$$

The complexity of the expression PDF of G-G for Meijer's G function [27]. In [15], the PDF of G-G provides a better fit for experimental results. Table 1 shows a comparison of gamma values for various levels of air turbulence.

Table 1,
Comparison of G-G values for different ATs.

Performance parameters	Weak turbulences	Moderate turbulences	Strong turbulences
σ_R^2	0.3	1.5	3.4
β_o	10.1	4.1	4.3
α_o	11.6	1.8	1.5

3.3 Nakagami-m Distribution

The Nakagami (N) -m distribution channel is a versatile statistical mode that ranges from weak to strong. A probability density model connected to the G-G distribution is the N distribution. The N channel model performs better than the Rayleigh model due to two parameters: the shape parameter M and the regulating spread **Ω** [15]. The PDF for the Nakagami fading model is given by:

$$P(I_o)_{Nd} = \frac{2M^M I_o^{2M-1}}{\Gamma(M)} \exp\left(\frac{-M I_o^2}{2\Omega}\right), I_o > 0 \quad \ldots(7)$$

where $\Gamma(M)$ is the Gamma function, M is the particle's shape parameter, ($M \geq 0.5$), **Ω** is used to control the spread of the distribution, **Ω** =E $\{I_o^2\}$

$$M = \frac{E^2\{I_o^2\}}{E\{[I_o^2 - E(I_o^2)]\}^2} \quad \ldots(8)$$

3.4 Málaga M Distribution

A PDF representation of the optical radiation distribution across the Malaga Canal in the FSO link can be represented as follows: [29]

$$P(I_o)_M = \vartheta \sum_F^{\beta_o} \alpha_{oF} (I_o)^{\frac{\alpha_o+F}{2}} B_{\alpha_o-F}\left(2\sqrt{\frac{\alpha_o I_o F}{PF+\eta}}\right) \quad \ldots(9)$$

$$\vartheta \triangleq \frac{2(\alpha_o)^{\frac{\alpha_o}{2}}}{(P)^{1+\frac{\alpha_o}{2}}\Gamma(\alpha_o)}\left(\frac{P\,F}{P\,F+\eta}\right)^{F+\frac{\alpha_o}{2}} \quad \ldots(10)$$

$$\alpha_{oF} \triangleq \binom{\beta_o - 1}{F-1}\frac{(PF+\eta)^{1-\frac{F}{2}}}{(F-1)!}\left(\frac{\eta}{P}\right)^{F-1}\left(\frac{\alpha_o}{F}\right)^{\frac{F}{2}} \quad \ldots(11)$$

Where P, F, and η are the average power of the scattering component, the value of the fading parameter, and the average power of the LOS component**,** respectively.

3.5 Negative Exponential Distribution

One more model that has gained widespread acceptance for use in the simulation of highly turbulent environments is the negative exponential (NE**)** distribution. This model, in conjunction with the Rayleigh distribution, is primarily used to test experimentally when there is an amplitude variation across the turbulent medium in the saturation area with regard to irradiance. This distribution's PDF file has been assigned as : [30]

$$P(I_o)_{NE} = \frac{1}{I_o}\exp), \quad , I_o > 0 \quad \ldots(12)$$

Where $E\{I\} = I_o$ the mean of the receiver optical irradiance.

3.6 Inverse-Gaussian Distribution

Inverse-Gaussian (I-G) distribution is modeled as an alternative to LN distribution and is usually utilized for weak atmospheric turbulence conditions. The I-G channel model's PDF is as follows [31]:

$$P(I_o)_{Nd} = \sqrt{\frac{\lambda}{2\pi}} I_o^{-3/2} \exp\left(\frac{-\lambda(1-\mu)^2}{2\mu^2 I_o}\right), I_o > 0 \quad \ldots(13)$$

Where λ>0 is the distribution scale parameter and $\mu > 0$ parameter of mean fluctuations.

3.7 K-Distribution

The K-distribution was used to model a severely weathered communication channel in the FSO link [29]. The exponential and G-G distribution models are combined to form the K distribution. When

compared to the NE model, this model is most frequently utilized for conditions of significant air turbulence, and its practical findings are quite consistent with its theoretical predictions. A search was performed on FSO communications implemented through atmospheric disturbance channels for the distribution of K and it has been demonstrated that an accurate approximation of the PDF of the K distribution can be obtained by summing a limited number of weighted negative exponential PDFs as: [33]

$$P(I_o)_K = \frac{2\alpha_o^{\frac{\alpha_o-1}{2}}}{\Gamma(\alpha_o)} I_o^{\frac{\alpha_o-1}{2}} B_{\alpha_o-1}\left(2\sqrt{\alpha_o I_o}\right), I_o > 0 \quad ...(14)$$

When β is unity, the G-G distribution reduces to K-distribution. Likewise, the K-distribution tends to NE distribution when $\alpha \to \infty$ [34].

3.8 Fisher–Snedecor F Distribution

The channel gain for the FSO link is modeled as:

$$h = h^{PL} h^{AT} h^{PE} \quad ... (15)$$

Where $h^{PL}, h^{AT}, \text{and } h^{PE}$ are deterministic propagation loss, AT attenuation, and PE, respectively. A PDF of atmospheric turbulence can be represented for both links as: [26]

$$f_{h^{AT}}(x) = \frac{\Gamma(\alpha+\beta)\alpha^{\alpha}(\beta-1)^{\beta}x^{\alpha-1}}{\Gamma(\alpha)\,\Gamma(\beta)(\alpha x+\beta-1)^{\alpha+\beta}} \quad ... (16)$$

Where α and β are two variables that are the internal and external measures of disturbance, respectively. Hence, they have an important role in affecting the optical propagation properties of the link, where

$$\alpha = \frac{1}{\exp(\sigma_{Inn}^2)-1} \quad ... (17)$$

$$\beta = \frac{1}{\exp(\sigma_{Inm}^2)-1} + 2 \quad ... (18)$$

Where, σ_{Inn}^2 and σ_m^2 are the small-scale and large-scale log-irradiance variances, respectively, where σ_{Ins}^2 can be expressed as:

$$\sigma_{Inn}^2 = \frac{0.51\delta_{SP}^2(1+0.69\delta_{SP}^{\frac{12}{5}})^{-5/6}}{1+0.90d^2(\frac{\sigma}{\delta_{SP}})^{12/5}+0.62d^2\sigma^{12/5}} \quad ... (19)$$

Where $\delta_{SP^2}$is the spherical scintillation index (SSI) of the FSO link, σ^2 represents the strength of irradiance fluctuations, and d is the equivalent aperture diameter. Such turbulence [26]. Moreover, σ_L^2 can be expressed as:

$$\sigma_m^2 = \sigma_m^2(I_0) - \sigma_m^2(L_0) \quad ... (20)$$

Where $\sigma_m^2(I_0)$ and $\sigma_{Inm}^2(L_0)$ are the inner and outer large-scale log-irradiance variances, the line-of-sight path for D2D communication is critical in maintaining a reliable wireless optical communication link. Therefore, the dangers that may occur due to the movement of the source or interface or the deviation of the path is taken into account. That causes optical beam routing errors and data loss. In addition, The PDF of the pointing error can be expressed as:

$$f_{h^{PE}}(x) = \frac{\mathcal{E}^2}{A^{\mathcal{E}^2}} y^{\mathcal{E}^2-1}, 0 \le y \le A \quad ... (21)$$

Where the A is a fraction of power at the receiver. Here, $\mathcal{E} = \frac{\omega^{zeq}}{\sigma^{\mathcal{E}}}$, Where ω^{zeq} and $\sigma^{\mathcal{E}}$ are the beam-width and the PE displacement standard deviation, respectively. The PDF of the instantaneous SNR is represented as follows over the Fisher–Snedecor F composite fading channel: [35]

$$P(I_o) = \frac{\eta^m P^{m-1}}{B_e(m,n)(\eta P+1)^{m+n}} \quad ... (22)$$

Where $\eta = \frac{m}{(n-1)\overline{p}}$ The multipath fading intensity is denoted by m and n values. denotes the shadowing shape parameter, $\overline{p}$ is the average SNR, and $B_e(\cdot,\cdot)$ denotes the beta function.

4. Kullback–Leibler Divergence

The congruence between the mathematical analysis and the actual experimental data observed among [9] of these PDFs is a necessary factor in choosing the most appropriate distribution for channel modeling, as well as the computational complexity factor, which is the main point of this paper.

The best PDF is determined to be the one with the least amount of spacing to Kullback–Leibler divergence (KLD) metrics [9], which enables a performance metric to be computed for each candidate PDF. KLD is most helpful for application in a real-world dataset from a practical standpoint because it directly provides specific outputs that make it possible to scan any PDF file. KLD is a way to gauge how close two probability distributions are. Let P_1 and P_2 be two distinct distributions defined on the same probability space, where P_1 is a theoretical probability distribution and P_2 is measured against an experimental KLD between two distributions is given as:

$$D_{KLD}(P_1||P_2) = \sum_n P_{1n} \log_2 \frac{P_{1n}}{P_{2n}} \quad ...(23)$$

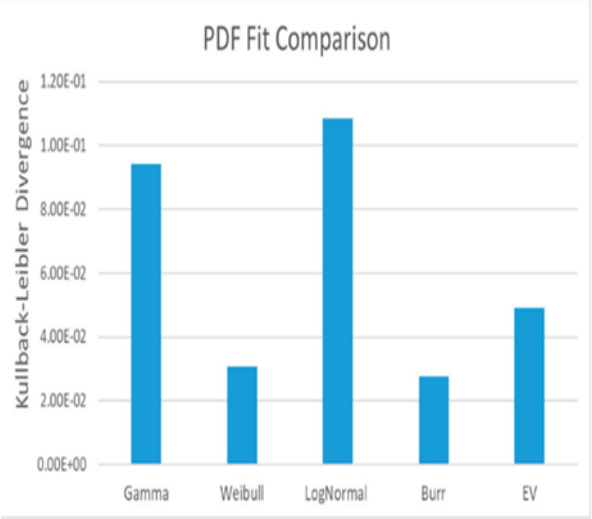

Fig. 3. The Kullback–Leibler divergence values.

The best result we want to achieve is that the convergence between p and q occurs when KLD decreases. And The KLD is non-negative and asymmetric in P_1 and P_2 [9]. The results from Figure 3. indicate that the distribution of LN is the worst in agreement with the experimental data ($D_{KLD} = 1.09 \times 10^{-1}$), then it is followed by G-G.

On the contrary, when the value of KLD approaches zero, the Burr distribution is the best among them ($D_{KLD} = 2.77 \times 10^{-2}$) followed by the Weibull distribution. Despite the importance of KLD in selecting the most appropriate channel distributions based on the PDF for each distribution, we focused on choosing the model with the least computational complexity. It should be noted that we pay attention to the design of the model and the amount of its estimation of the various channel disturbances. Although the Burr and Weibull model is the closest to matching, the F model is the most accurate, least complex, and sequential in mathematical terms, similar to the LN, G-G, and M distributions, as it was proven in [23].

5. Numerical Results and Discussions

This section analyzes the efficacy of the PDFs through simulations. To compare the effectiveness of models for FSO channels under different ATs. Since atmospheric turbulence strongly affects the FSO channel, channel modeling is necessary to match it in simulation. We do not have a guarantee of the stability of weather fluctuations, as they are likely to change at any moment. Therefore, PDF models require accuracy in an arithmetic expression, simplicity in analysis, and obtaining satisfactory results that match the reality of simulation to ensure reliable results for choosing the most appropriate model for FSO channel modeling in different channel conditions.

Figure 4 displays the log-normal pdf versus log-irradiance variance for various values. σ_o^2 The distribution becomes more lopsided as the value of σ_o^2 increases, with longer tails extending in an infinite direction. We chose three values of σ_o^2 (0.2, 0.5, and 0.8). This indicates the degree to which their fluctuation changes as the channel inhomogeneity continues to increase.

According to Figure 5, there are three different levels of turbulence: weak, moderate, and strong. The figure demonstrates that as the turbulence increases from the weak to the strong regime, there is a corresponding increase in the range of potential values of the irradiance. The distribution becomes more spread as a result.

The results are shown in Fig. (6 and 7) for channel parameters G-G distribution, where the simulation was done assuming strong and medium turbulences. In addition to a distance of 4500 meters between the transmitter and the receiver at λ =1550e-9. Under strong turbulence, the amount of radiation at a distance of 1840 meters is -30.73dB, and this amount decreases as the distance of the FSO connection increases due to the attenuation of weather conditions affected by an amount change in the refractive index, as it is -35.36dB at approximately 5514 meters. we noticed (fig. 7) the G-G model under almost medium conditions, the signal radiation is -5.21dB at a distance of 1741 meters. Now, it is clear to us from (fig 6,7) that weather conditions have an essential and sensitive impact on the design of the FSO link, which requires accurate modeling in estimating the system parameters.

In Figure 8, a lower standard deviation results in a narrower distribution. When the values of the variable irradiance become closer to the mean, there will probably be less variability. Therefore in Fig.9, A large value of M close to 1 is tested in the Nakagami-m distribution, and signal crossovers are reduced, resulting in a more stable channel with less deep fade. As a result, Nakagami-m Model has become more similar to an R distribution

where we look at the F distribution (Fig. 10), and we find that it approximates the radiation distribution to the G-G distribution within different magnitudes of the channel parameters. This is what suits us in choosing the most appropriate mathematical analysis in line with different weather conditions.

In Figure 11, the increase in the irradiance values of NE distribution produces a greater degree of fluctuation in the channel coefficients, which in turn leads to an increase in the turbulence level. In Figure 12, the simulation results for various values of the σ parameter are presented. As it can be seen, the performance improves as the value increases.

After conducting mathematical analysis and simulation, it was found that each distribution has its own characteristics that distinguish it in terms of channel parameters, the intensity of disturbance, the accuracy of matching with experimental reality, and computational complexity in modeling the FSO channel. We found that R, LN, I-G, N, NE, and K distributions are not suitable for channel different conditions, though accurate and appropriate to certain circumstances. As for the G-G and F distributions, we consider them the most appropriate for achieving more benefit for modeling the channel under different conditions.

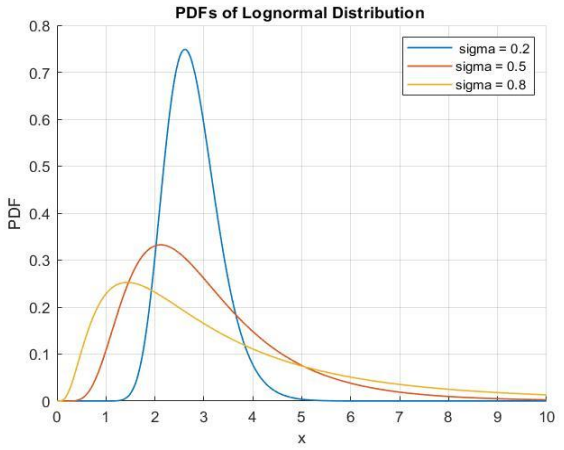

Fig. 4. PDF of Lognormal Distribution Under Weak AT.

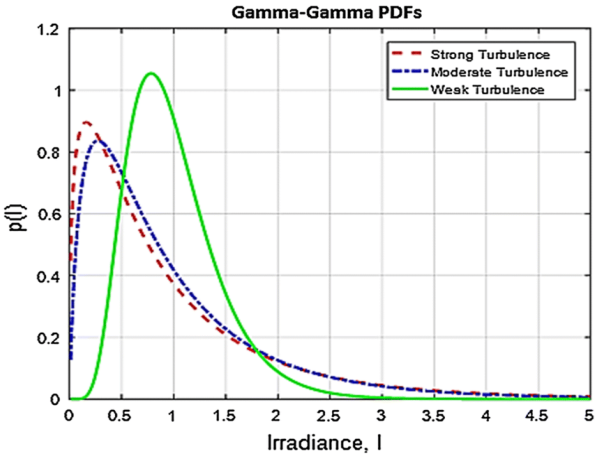

Fig. 5. PDF of Gamma-Gamma Distribution Under Different ATs.

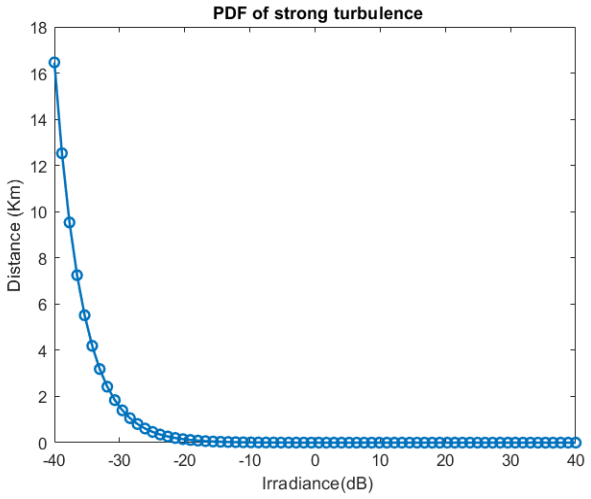

Fig. 6. Irradiance and Distance of Gamma-Gamma Distribution Under Strong A

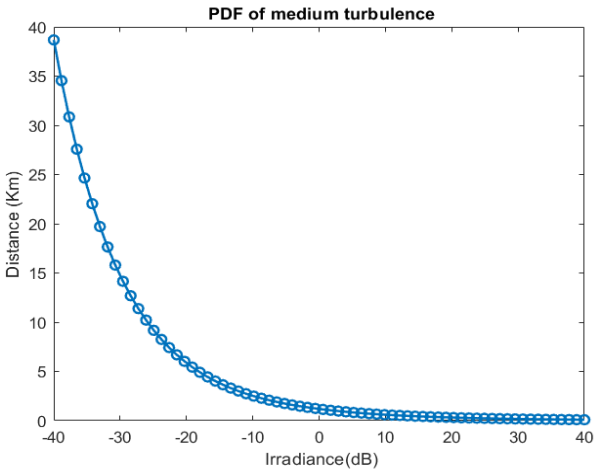

Fig. 7. Irradiance and Distance Gamma-Gamma Distribution Under Medium AT.

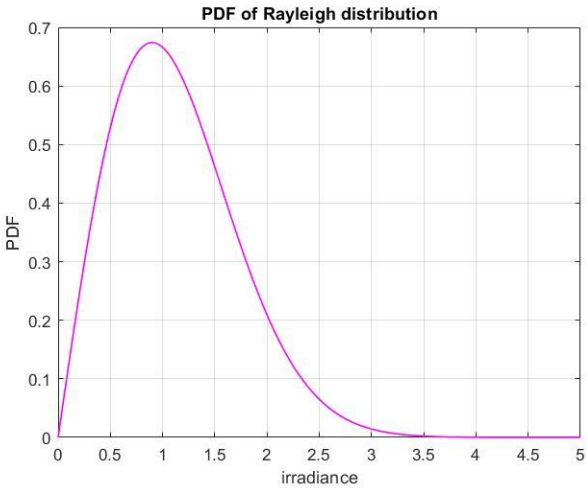

Fig. 8. PDF of Rayleigh (R) Distribution.

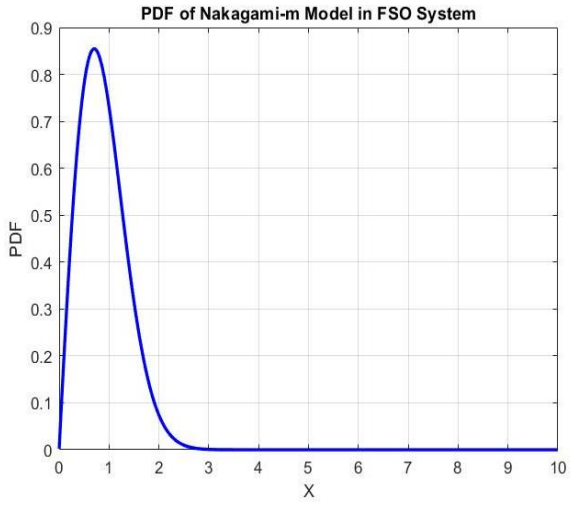

Fig.9. PDF of Nakagami-m Model.

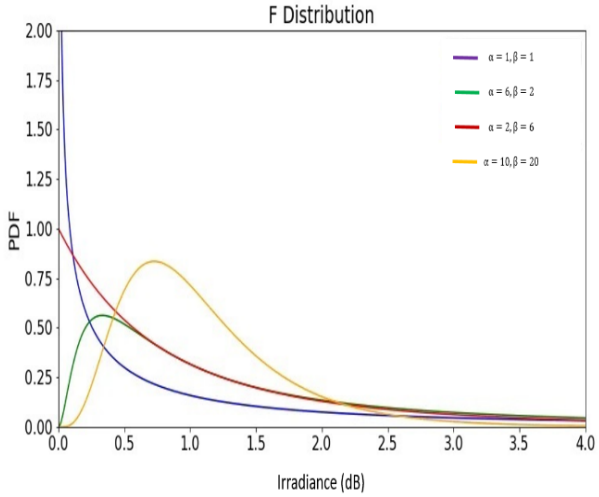

Fig. 10. PDF of Fisher- Snedecor F distribution.

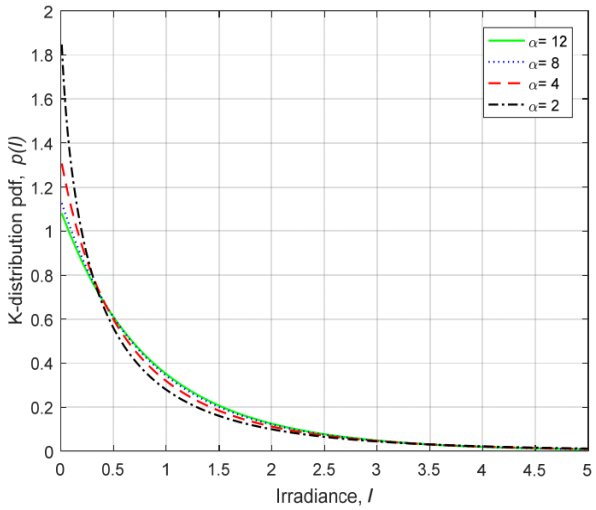

Fig.11. PDF of K-Distribution.

A PDF was calculated for both distributions (G-G and F) for different parameters under similar conditions, as in Figure 13. In comparison to distribution 1, PDF 2 for both distributions has a somewhat smaller shape parameter, indicating a relatively lighter tail. If it is clear from the figure, the experimental correspondence in the curves between the (G-G and F) distributions, despite the slight difference, may not be effective in terms of practice.

In summary, the LN model is not suitable for practice. Although LN is very simple to distribute, when comparing the LN model to the observed data under weak perturbation conditions, it performs imprecisely in the tails of the PDF. Although I-G the distribution is simple in mathematical representation.

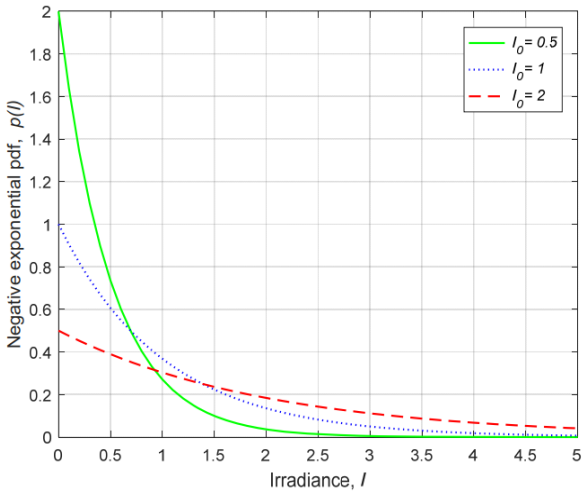

Fig. 12. PDF of Negative Exponential (NE) Distribution.

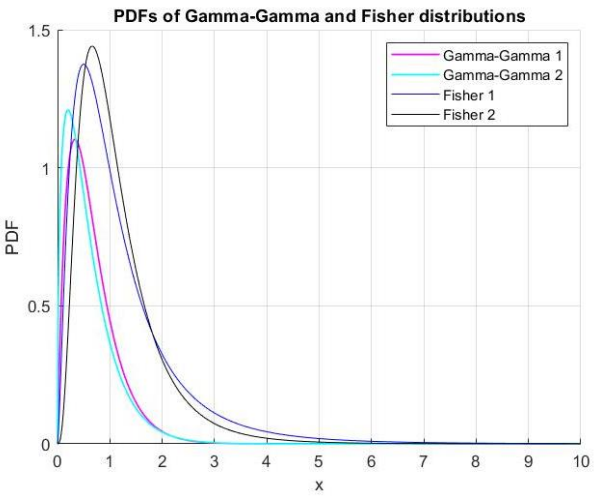

Fig. 13. Correspond PDF of Gamma-Gamma and Fisher- Snedecor F Distributions.

The I-G distribution fits a value closer to the LN model than the G-G distribution model. The NE distribution and the G-G model have the same ranges, but the drawback of the former is that the optimal value occurs in the negative region. On the other hand, the main advantage of the G-G model is its ability to work well in situations where other channels struggle due to the effects of sub-channel correlation, even in cases of wide perturbation variations.

In addition, regarding the G-G distribution, we find the expression complexity of the Meijer function G, which generates additional computational complexity. However, it is suitable for potential conditions within the proposed system, which range from medium to strong, and we consider it to be the most suitable type for estimating channel parameters. Also, the distribution of F is the simplest for the same expected results at the G-G distribution.

6. Conclusions

Speed and high data flow are prerequisites for the current and later generations of communication systems. To meet this demand, Communications FSO has emerged as a primary candidate because of its ability to bypass frequency-related licensing restrictions, its relative ease of installation, interference reduction, and cost-effectiveness. However, the main challenge is maintaining connection reliability, primarily due to adverse weather conditions. Various factors, such as luminescence refractive index and PEs affect the performance of optical signals. To address these limitations, we performed an analysis of PDFs from different types of channel models used in FSO communications to calculate channel states under different perturbations. PDF plays a critical role in testing the appropriate design of potential cores of FSO systems. Therefore, we considered common FSO channel modeling distributions, such as Rayleigh, lognormal, Málaga, Nakagami, K-distribution, Negative-Exponential, Inverse-Gaussian, Gamma-Gamma, and fishier F distributions. Our analysis revealed that the LN, R, N, and I-G distributions exhibit simple mathematical and experimental properties, which makes them suitable for weak weather conditions. On the contrary, the M, F, and G-G distributions showed better performance under different conditions, especially under strong weather conditions. The M distribution, although empirically appropriate, has greater mathematical complexity. On the other hand, the F distribution showed the simplest mathematical analysis with satisfactory results. Finally, the G-G distribution emerged as the most suitable choice among all species, performing well in all regimes, ranging from weak to strong turbulent regions. As a result, we recommend using the gamma-gamma distribution as a channel model for FSO communications based on channel analysis using PDF distributions. This choice ensures robust performance and reliability under changing weather conditions.

Abbreviations

AT	Atmospheric Turbulence
BER	Bit Error Rate
D2D	Device to Device
F	Fisher- Snedecor F
FSO	Free Space Optical
G-G	Gamma-Gamma
I-G	Inverse-Gaussian
KLD	Kullback–Leibler Divergence
LN	Lognormal
LOS	Line-of-Sight
N	Nakagami
NE	Negative Exponential
M	Málaga
MGF	Meijer's G Function
MIMO	Multiple Input Multiple Output
PDF	Probability Density Function
PE	Pointing Error
SNR	Signal to Noise Ratio
SSI	Spherical Scintillation Index

7. References

[1] Mohammed Jawad Al-Dujaili et al.," FifGenerationTelecommunicationsTechnologies: Features, Architecture, Challenges, and Solutions," Wireless Personal Communications volume 128, pages447–469 (2023).

[2] Omar Aboelala et al., "A Survey of Hybrid FreeSpace Optics (FSO) Communication Networks to Achieve 5G Connectivity for Backhauling", Entropy 2022, 24(11), 1573.

[3] Omar Hayat et al., "In-Band Device to Device (D2D) Communication and DeviceDiscovery: A Survey", Wireless PersonaCommunications volume 106, pages451–472 (2019).

[4] Kavita and Jagtar Singh," MATLAB Based Simulink Modeling and Performance Analysis of Free Space Optical

Communication System", Journal of Online Engineering Education ISSN: 2158-9658 Volume: 13 Issue: 2, 24 November 2022.

[5] Ayad Atiyah Abdulkafi et al., "Multilayered optical OFDM for high spectral efficiency in visible light communication system," Photonic Network Communications volume 38, pages299–313 (2019).

[6] Iman Hadi Abdulameer, Rawaa Dawoud Al-Dabbagh "Self-adaptive Differential Evolution based Optimized MIMO Beamforming 5G Networks" Iraqi Journal of Science, 2022, Vol. 63, No. 63. 8, pp: 3628-3639DOI:10.24996/ijs.2022.63.8.37.

[7] Osamah S. Badarneh et al., "Performance Analysis of FSO Communications Over F Turbulence Channels with Pointing Errors", IEEE COMMUNICATIONS LETTERS, Vol. 25, NO. 3, p. 926–930, Mar. 2021.

[8] Panagiotis J. Gripeos et al., "Time and Spatial Jitter Influence on the Performance of FSO Links with DF Relays and OC DiversityOverTurbulenceChannels," Photonics2021,8(8),318; https://doi.org/10.3390 /photonics8080318.

[9] Antonios Lionis et al," RSSI Probability Density Functions Comparison Using Jensen-Shannon Divergence and Pearson Distribution", Technologies 2021, 9(2),26; https://doi.org/10.3390/technologies9020026.

[10] Abdullah.A.Abdullah1 et al., "New Modulation Method in FSO Communication Using Different Wavelengths (650,532,405) nm in the Iraqi Weather", Iraqi Journal of Science, Vol. 59, No.1A, pp: 233-239, 2018. http://DOI:10.24996/ijs.2018.59.1A.25.

[11] Dubey, D. et al., "Error performance analysis of PPM- and FSK-based hybrid modulation schme for FSO satellite downlink". Opt. Quant. Elect. 2020, 52, 286.

[12] Noor Wisam Sabri, Firas S. Mohammed, "Multi-channel Optical Wireless Communication under the Effect of Low Electric Field", Al-Mustansiriyah Journal of Science, Volume 33, Issue 2, 2022.

[13] Bobby Barua et al., "Performance Evaluation of Different Type of Channel Models in FSO Communication" International Journal of Science and Advanced Technology, Volume 1 No 5 July 2011

[14] Ayshah S. Alatawi, "Effects of Atmospheric Turbulence on Optical Wireless Communication in NEOM Smart City", Photonics 2022, 9, 262. https://doi.org/10.3390/photonics9040262.

[15] Anandkumar et al., "A survey on performance enhancement in free space optical communication system through channel models and modulation techniques" , Opt Quant Electron 53, 5 (2021). https://doi.org/10.1007/s11082-020-02629-6.

[16] Z. Ghassemlooy et al, "Free-space optical communication using subearrier modulation in gamma-gamma atmospheric turbulence," ICTON '07, vol. 3, pp. 156 - 160, 1 - 5 July 2007

[17] Yan Wu et al.," Performance Analysis of a Multi-Hop Parallel Hybrid FSO/RF System over a Gamma–Gamma Turbulence Channel with Pinting Errors and a Nakagami-m Fading Channel" Photonics 2022, 9, 631.

[18] Lwaa Faisal Abdulameer, Hala Fadhil," Performance Analysis of FSO under Turbulent Channel Using OSTBC", Al-Nahrain Journal for Engineering Sciences (NJES) Vol.2 No.3, 2018, pp.344-349, http:/ /doi.org/10.29194/NJES.21030344.

[19] Jaiswal et al., "Differential optical spatial modulation over atmospheric turbulence. IEEE J.Sel. Top. Signal Process. 2019, 13, 1417–1432.

[20] K. Peppas et al., "The Fisher-Snedecor F distribution model for turbulence-induced fading in free-space optical systems," J. Lightw. Technol., vol. 38, no. 6, p. 1286–1295, Mar. 2020.

[21] Mahmoud Yasser et al., "Impact of nonzero boresight and jitter pointing errors on the performance of M-ary ASK/FSO system over Málaga (M) atmospheric turbulence", Optical and Quantum Electronics volume 53, Article number: 46 (2021).

[22] Yi Wang and Rui Zhou," Performance Study of Generalized Space Time Block Coded Enhanced Fully Optical Generalized Spatial Modulation System Based on Málaga Distribution Model", Photonics 2023, 10, 285.

[23] Ansari, I.S.; Yilmaz, F.; Alouini, M.-S. Performance Analysis of Free-Space Optical Links Over Malaga (M) Turbulence Channels with Pointing Errors. IEEE Trans. Wirel. Communicate. 2016, 15, 91–102

[24] Myoungkeun Shin," Statistical Modeling of the Impact of Underwater Bubbles on an Optical Wireless Channel", IEEE Open Journal of the Communications Society

[25] (Volume: 1), Page(s): 808 – 818, 19 June 2020.

[26] Wafaa Mohammed Ridha Shakir, Mohammed-Slim Alouini," Secrecy Performance Analysis of Parallel FSO/mm-wave System Over Unified Fisher-Snedecor Channels", IEEE Photonics Journal (Volume: 14, Issue: 2, April 2022)

[27] Manh Le-Tran, Sunghwan Kim, "Performance Analysis of Dual-Hop FSO Cooperative Systems over F Turbulence with Pointing Errors", Photonics 2022, 9, 437. https://doi.org/10.3390/photonics9070437.

[28] Zixuan Xu et al.," BER and Channel Capacity Performance of an FSO Communication System over Atmospheric Turbulence with Different Types of Noise", Sensors 2021, 21, 3454. https://doi.org/10.3390/s21103454.

[29] Yoo, S.K, et al., "The Fisher-Snedecor F distribution: A simple and accurate composite fading model. IEEE Community. Lett. 2017, 21, 1661–1664.

[30] Akinchan Das et al.," Free space optical links over Málaga turbulence channels with transmit and receive diversity", Optics Communications 456 (2020) 124591

[31] Z. Ghassemlooy, et al," Optical wireless communications system and channel modeling with MATLAB, CRC Press, NY, 2013.

[32] Sun, H. et al.," Computationally tractable model of energy detection performance over slow fading channels" IEEE Commun. Lett. 14(10), 924–926 (2010).

[33] S. Tannaz et al.," Impacts of the negative-exponential and the K-distribution modeled FSO turbulent links on the theoretical and simulated performance of the distributed diffusion networks", Journal of Communication Engineering, Vol. 8, No. 2, July-December 2019.

[34] Hossein Samimi et al.," Subcarrier Intensity Modulated Free-Space Optical Communications in K-Distributed Turbulence Channels", Journal of Optical Communications and Networking (Volume: 2, Issue: 8, August 2010).

[35] Aladeloba et al," Improved bit error rate evaluation for optically pre-amplified free-space optical communication systems in the turbulent atmosphere", IET Optoelectron. 6(1), 26–33 (2012)

[36] Weijun Cheng, et al., "On the Performance Analysis of Switched Diversity Combining Receivers over Fisher–Snedecor F Composite Fading Channels", Sensors 2021, 21, 3014. https://doi.org/10.3390/s21093014.

مقارنة دالة كثافة الاحتمال بناءً على نماذج قناة FSO مختلفة في ظل اضطرابات جوية مختلفة

مهدي عبد عطية * لواء فيصل عبد الامير **
غوراف نارخيدل***
*،**قسم هندسة المعلومات والاتصالات / كلية الهندسة الخوارزمي / جامعة بغداد/ العراق*
*** كلية هندسة الإلكترونيات والاتصالات/ جامعة السلام العالمي بمعهد ماساتشوستس للتكنولوجيا/ الهند*
*البريد الالكتروني :mahdi.abd2103m@kecbu.uobaghdad.edu.iq
**البريد الالكتروني:lwaa@kecbu.uobaghdad.edu.iq
***البريد الالكتروني :ggnarkhede9@gmail.com

الخلاصة

في الآونة الأخيرة، أصبحت بيئات الاتصال اللاسلكي ذات السرعات العالية والتعقيد المنخفض أمرًا أساسيًا. ظهرت التقنية البصرية في المجال الفضائي الحر (FSO) كحلاً واعدًا لتوفير اتصالات مباشرة بين الأجهزة في إعدادات الاتصال اللاسلكي عالية التردد. ومع ذلك، فإن اتصالات FSO عُرضة لتقلبات إشارة ناجمة عن الطقس، مما يؤدي إلى انحسار الإشارة وضعفها عند المستقبل. للتغلب على هذا التحدي، تم اقتراح عدة نماذج رياضية لوصف الانتقال من التضخم الجوي الضعيف إلى القوي، بما في ذلك توزيعات Rayleigh و lognormal و Málaga و Nakagami-m و K-distribution و Weibull و Negative-Exponential و Inverse-Gaussian و G-G و Fisher Snedecor Fفي هذه الورقة، ندرس ونحلل بشكل موسع مختلف الدوال الكثافة الاحتمالية (PDFs) التي تحكم قناة FSO، مع النظر في نماذج القنوات المختلفة. الهدف هو توفير فهم شامل لكيفية تصميم قنوات FSO بفعالية باستخدام PDFs المختلفة. النمذجة الدقيقة ضرورية لتصميم أنظمة FSO يمكن أن تعمل بشكل مثلى تحت ظروف بيئية محتملة. اختيار النموذج الصحيح لل PDF الذي يلعب دورًا حاسمًا في تحديد أداء قناة FSO أثناء تصميم النظام. من خلال العديد من نماذج PDF المتاحة، يهدف هذا الدراسة إلى تحديد النموذج الأكثر فعالية للاستخدام في نمذجة قناة FSO.